Brain infiltration of breast cancer stem cells is facilitated by paracrine signaling by inhibitor of differentiation 3 to nuclear respiratory factor 1

Quentin Felty (feltyq@fiu.edu)
Florida International University Robert Stempel College of Public Health and Social Work
https://orcid.org/0000-0002-7151-0441

Jayanta K Das
Florida International University Robert Stempel College of Public Health and Social Work

Alok Deoraj
Florida International University Robert Stempel College of Public Health and Social Work

Deodutta Roy
Florida International University Robert Stempel College of Public Health and Social Work

Research Article

Keywords: NRF1, breast cancer metastasis, ID3, cancer stem cells

Posted Date: March 22nd, 2022

DOI: https://doi.org/10.21203/rs.3.rs-1443283/v1

Abstract

Treatment options for brain metastatic breast cancer is limited because the molecular mechanism for how breast cancer cells infiltrate the brain is not fully understood. In order for breast tumors to metastasize to the brain first cells need to detach from the primary tumor, enter in the blood circulation, survive within the microvascular niche, and then cross the blood brain barrier (BBB) to colonize into the brain. It is critical to understand how breast cancer cells transmigrate through the BBB to prevent brain metastasis. Nuclear respiratory factor 1 (NRF1) transcription factor has been reported to be highly active in several human cancers and its aberrant expression facilitates in the acquisition of breast cancer stem cells (BCSCs). Inhibitor of differentiation protein 3 (ID3), a transcription regulating protein, induces pluripotent endothelial stem cells (ESCs). Herein we investigated if NRF1-induced BCSCs could cross a BBB model and guiding of BCSCs by ID3-induced ESCs across the BBB. BCSCs and ESCs were subjected to functional gain/loss experiments to determine if NRF1/ID3 contributed to lineage specific BCSCs organ entry. First, we tested whether NRF1 promoted migration of breast cancer using a BBB model consisting of BCSCs or MDA-MB231 cells, brain endothelial cell layer, and astrocytes. NRF1 overexpression increased the propensity for BCSCs and NRF1-induced MDA-MB231 cells to adhere to brain endothelial cells and migrate across a human BBB model. Increased adhesion of NRF1 induced BCSCs to $ESCs^{ID3}$ was detected. NRF1 induced BCSCs crossed through the BBB model and this was promoted by $ESCs^{ID3}$. We also showed that environmental relevant exposure to PCBs (PCB153 and PCB77) produced differential effects. Treatment with PCB153 showed increased growth of NRF1 induced BCSCs tumor spheroids and increased in vivo migration of $ESCs^{ID3}$. Exosomal ID3 released from endothelial cells also supported the growth of NRF1 induced BCSCs and provide the basis for paracrine effects by $ESCs^{ID3}$ associated with breast tumors. Xenograft experiments showed that ID3 overexpressing brain ESCs not only supported the growth of BCSC tumorospheroids but guided them to the neural crest in zebrafish. These findings show for the first time a novel role for ID3 and NRF1 by which $ESCs^{ID3}$ help guide $BCSCs^{NRF1}$ to distant metastatic sites where they most likely facilitate the colonization, survival, and proliferation of BCSCs. This knowledge is important for pre-clinical testing of NRF1/ID3 modifying agents to prevent the spread of breast cancer to the brain.

Introduction

Nuclear respiratory factor 1 (NRF1) is a pioneer transcription factor that localizes to several thousand sites in the human genome. Our research has shown that NRF1 motif sequence-enriched genes are involved in ER/PR negative HER2 positive breast cancer signaling pathways (1). NRF1 mRNA and protein levels including NRF1 transcriptional activity were significantly higher in ER/PR- HER2 + breast cancer samples compared to normal breast tissues. Moreover, our novel research showed that NRF1 drives estrogen-dependent breast tumorigenesis. Overexpression of NRF1 combined with exposure to a carcinogenic dose of 17β-estradiol (E2) generated breast tumor initiating cells (BTICs) or breast cancer stem cells (BCSCs) that formed tumors in vivo (2). The capability of circulating tumor cells to form metastatic lesions depends on multi-lineage potential and self-renewal (3). Distant organ breast cancer

metastasis also appears to rely on a specific subpopulation of estrogen receptor negative (ER-) breast cancer cells. For instance, triple negative MDA-MB231 breast cancer cells that disseminate to the lung, bone, liver, and brain in NOD-SCID mice are specific subclones of the parental line (4). Our research findings of NRF1 inducing more than 10 distinct BCSC subtypes supports the idea of different tumor cell fates that render them increasingly competent to establish metastatic lesions in specific organs (2).

The inhibitor of DNA binding and differentiation (ID) family of proteins are transcription regulators also reported to support breast cancer metastasis (5, 6). ID3 is part of the ID family of proteins that are expressed by embryonic and somatic stem cells; and contribute to stemness by enhancing proliferation and inhibiting differentiation. Our research has shown that exposure to E2 and PCB153 increased ID3 phosphorylation and levels of ID3 protein in endothelial cells (7–9). Moreover, stable ID3 overexpression induced endothelial stem cells ($ESCs^{ID3}$); and $ESCs^{ID3}$ exposed to E2 and PCB153 generated vascular spheroids and sprouting (10). The prevalence of breast cancer metastasis to the brain is reported to be 10–16% (11). Survival of circulating tumor cells or micrometastases is made difficult because of the absence of environmental cues from the breast tissue niche and passage across the blood brain barrier. Whether $ESCs^{ID3}$ may help BCSCs adapt to a new microenvironment and facilitate distant organ metastasis is not known. Elevated circulating endothelial progenitor stem cells have been reported in breast cancer patients and were predictive of poor outcomes (12). Because ESCs may support survival of BCSCs and adhesion to the blood brain barrier, we propose that $ESCs^{ID3}$ facilitate the guidance of BCSCs to secondary target organs. The purpose of this study was to examine if NRF1 induced BCSCs could cross a model of the blood brain barrier as well as the contribution of $ESCs^{ID3}$ in guiding BCSCs across this barrier. Insight into mechanisms regulating specification and guidance that make BCSCs move to and grow in the distant organs will have significant clinical implications for breast cancer prevention and treatment and lay the groundwork to develop novel personalized breast cancer therapies based on paracrine NRF1-ID3 signaling.

Methods

Cell Lines: The MCF-10A and MDA-MB231 cell lines were received from American Type Culture Collection (ATCC, Manassas, VA, USA) and MCF-10A and MDA-MB231 cells were transfected with vector or cMV-NRF1-GFP construct (RG220113, OriGene Technologies). The human cerebral microvascular endothelial cell line HCMEC/D3 was received from Dr. B. Weksler, Weill Medical College of Cornell University, NY (Weksler et al., 2005); and will be referred to as wildtype endothelial cells (EC^{WT}) to distinguish them from $ESCs^{ID3}$. Cells were maintained in DMEM-F12 media with B27® serum-free supplement. The astrocyte cells (AC) were obtained from ScienCell, Carlsbad, CA, USA and were maintained in DMEM-F12 with astrocyte growth supplement. Cells were cultured at 37°C in a humidified atmosphere with 5% CO_2. Cell treatments were in DMEM-F12 in the absence of serum and growth factors for 3 h. Thereafter, the cells were treated with PCB153 (2,2',4,4',5,5'-hexachlorobiphenyl) and PCB77 (3,3',4,4'-tetrachlorobiphenyl) for the different experimental time periods. The PCB congeners were obtained from AccuStandard (New

Haven, CT) and dissolved in dimethyl sulfoxide (DMSO). Equal volumes of DMSO as in PCB treatment group were used in vehicle control with less than 0.1% percentage of DMSO in each group.

Tumorospheroid Assays: Approximately 100–150 cells per well were seeded in an ultra-low attachment 96-well plate (Corning Inc., Lowell, MA, USA) for tumorigenic spheroid formation studies. Cells were suspended in serum-free DMEM/F12 (1:1) culture medium supplemented with B27. The effect of endocrine disrupting chemicals, PCB153 (60μM) and PCB77 (60μM) were treated on the day of seeding cells. Spheroids were grown for 8 days and 16 days in liquid culture. A total of 15 spheroids with a minimum diameter of 50 mm were counted in each experimental group. Data were analyzed by ANOVA; Tukey's HSD test was used for multiple comparisons. Cells obtained from spheroids were analyzed by immunofluorescence, FACS, or immunoblotting, as described previously (2).

Blood–brain barrier (BBB) model: We established an in vitro BBB model consisting of human ECs, breast cancer stem cells (BCSCs) and astrocyte cells (ACs). Briefly, MDA-MB231 or BCSCs^{NRF1} were placed on 1cm height P1000 sterile tip (cut at both ends) surrounded by coculture of AC: EC (1:1) with Matrigel (cat# 354230; BD Biosciences, Franklin Lakes, NJ, USA) diluted in DMEM-F12 with astrocyte medium. The tip was removed after 24h and the cells were grown in DMEM-F12 with astrocyte medium to study 3D invasive migration. For cell adhesion and microinvasion assay, AC were grown first in a monolayer for 24 h and the ESCs^{ID3} were grown as layer on top of AC for 24 h; and BCSCs were cultured on top of ESCs^{ID3} for 24h.

Cell adhesion and migration assay: For cell adhesion and tumorigenesis/spheroid formation assay, BCSCs were seeded on monolayer of ESCs^{ID3} (24h) in serum-free media for 3days. For the transmigration assay, BCSCs were seeded on a monolayer of ESCs^{ID3} (24h) in serum-free media in the upper chamber of a transwell insert (pore size: 8 μm; Corning, Corning, NY, USA); 10% FBS medium was added to the lower chamber as a chemoattractant. After 24h incubation, invaded cells were photomicrographed by Nikon confocal microscopy. Invaded cells were counted and scored from the lower chamber in triplicate.

Antibodies and immunoblotting: Analysis of protein expression was performed by immunoblotting as described previously (2). Western blots and were probed with the following antibodies: ID3 (Cal BioReagent) and β-actin (13E5, rabbit mAb #4970, Cell Signaling Technology, Inc.). Electrochemiluminescence (ECL) intensity of detected target proteins was imaged and quantified with a Bio-Rad Versa Doc instrument. All immunoblots were accomplished a minimum of three times for each experiment.

Exosome isolation: Total Exosome Isolation Reagent (Catalog number: 4478359, Thermofisher Scientific) were used with cell culture media to isolate and concentrate exosomal ID3 from cell culture media of ESCs^{ID3} cells with the following protocol. Briefly, the reagent is added to the cell media sample, and the solution is incubated overnight at 2°C to 8°C. The precipitated exosomes are recovered by standard centrifugation at 10,000 x g for 60 min. The pellet is then resuspended in PBS or similar buffer, and the exosomes are ready to use in further experiments with co-culture cell media for 7 and 10 days.

Fluorescence activated cell sorting (FACS) analysis: After the staining, the cells were washed twice with stain buffer (BD Pharmingen) and analyzed using a Guava easyCyte flow cytometer (Millipore). For staining, 1×10^6 cells were pelleted and incubated for 45 min at 4°C with the following antibodies: ID3 biotin-FITC and NRF1 conjugated PE for FACS analysis and data was analyzed with the Guava easyCyte™ using the CytoSoft software program according to the manufacturer's instructions.

Xenotransplant migration assay: Xenograft zebrafish embryo experiments were performed at Florida International University, in accordance with IACUC-approved protocols (Protocol Approval #: IACUC-19-091-CR01). WT -TU Zebrafish embryos (2-dpf) were purchased from the Zebrafish International Resource Center (ZIRC), University of Oregon facility. BCSCs and ESCs were xenografted in zebrafish using specific microinjection equipment. Experiments were conducted in triplicate, and they were incubated for an extra 72 hours at 30-32°C. Approximately, 500 cells were injected into the yolk using pulled glass needles and a micromanipulator. The spread of the GFP fluorescent dye labeled lung PCB153 treated ID3 overexpressing cells. Cell migration was captured by Nikon confocal microscopy for metastasis studies. All injected cells stained with the fluorescent dye, CellTracker™ CM-DiI (both GFP and non GFP cells) were observed in live zebrafish embryo. For BCSCs brain metastasis xenotransplantation in zebrafish embryo, BCSCs were xenografted in the zebrafish embryo (to observe metastatic spread of the GFP fluorescent dye labeled $BCSCs^{NRF1}$ through blood vessels from the site of injection to the region of secondary target organs. The photomicrographs were taken by Nikon confocal microscopy. Total cells injected were stained with the fluorescent dye, CellTracker™ CM-DiI (stained both GFP and non GFP cells).

Statistical Analyses: All statistics were performed using VassarStats statistical software (Richard Lowry, Poughkeepsie, NY, USA). One-way analysis of variance (ANOVA) was achieved to detect any differences between groups. If the result of the ANOVA was significant, pair wise comparisons between the groups were made by a post-hoc test (Tukey's HSD procedure).

Results

The initiation and progression of estrogen-induced breast tumors are proposed to arise from BTICs (13). We previously showed that stable NRF1 overexpression was responsible for the acquisition of BTICs from the human epithelial breast cell line MCF-10A (2). Overexpression of NRF1 combined with exposure to a carcinogenic dose of 17β-estradiol (E2) generated BTICs that formed tumors in vivo (2). These BTICs are referred to as $BCSCs^{NRF1}$. Transcription regulator ID3 is known to support the invasive growth of breast cancer cells and tumor initiating capacity of breast cancer metastases (5, 6). ID proteins have also been demonstrated to be secreted angiogenic transcription factors in arthritis, but whether endothelial ID3 may influence the growth of BCSCs is not known (14). We have shown that stable ID3 overexpression contributes in the acquisition of endothelial stem cells (10). Here, we determined whether $ESCs^{ID3}$ influence tumor spheroid growth of NRF1 induced BCSCs.

The $ESCs^{ID3}$ were generated as described previously (8). NRF1 induced BCSCs were co-cultured with either wild-type (EC^{WT}) or $ESCs^{ID3}$ for 16 days after treatment with vehicle control or PCBs (Fig. 1). Cells

were suspended in serum-free medium supplemented with B27. Approximately 100–150 cells per well were grown in ultra-low attachment plates. Cells were exposed to PCB congeners 77 and 153 on the day of seeding cells and spheroids were generated for 8 to 16 days in liquid culture. PCB153 treatment increased wildtype EC spheroid formation when compared to PCB77 (Fig. 1 row A). Exposure to both PCB congeners induced spheroid formation of NRF1 induced BCSCs (Fig. 1 row B). The paracrine effects of wildtype ECs on spheroid formation was determined by co-culturing with NRF1 induced BCSCs and/or astrocytes (Fig. 1 panel rows C-E). Co-culture of wildtype ECs with NRF1 induced BCSCs supported endothelial cell survival in PCB77 treatment compared to wildtype ECs alone (Fig. 1A). As shown in Fig. 1F, $ESCs^{ID3}$ (in green) contributed to larger spheroid formation when treated with PCBs compared to wildtype ECs (Fig. 1D,E).

Using the same experimental groups as described in Fig. 1, NRF1 induced BCSCs were co-cultured with wildtype ECs or $ESCs^{ID3}$ in a spheroid assay and diameters were measured for each group after 8 days and 16 days. PCB153 treatment showed an increase in wildtype EC spheroid growth compared to vehicle control at 8 and 16 days (Fig. 2 row A, F). NRF1 induced BCSCs did form tumor spheroids in control, however, PCB treated groups had larger spheroid diameters (Fig. 2 row B, F). As shown in Fig. 2C, BCSCs co-cultured with wildtype ECs had a similar phenotype to BCSCs cultured alone. Next, we cultured endothelial cells and astrocytes together with BCSCs (Fig. 2D, E). ID3 induced ESCs supported the growth of larger $BCSCs^{NRF1}$ tumor spheroids at 16 days (Fig. 2 row E, F) compared to wildtype EC (Fig 2. Row D). In summary, ID3 induced ESCs supported the growth of larger BCSCs tumor spheroids compared to wildtype ECs; and PCB153 treatment augmented the growth of BCSC tumor spheroids co-cultured with ID3 induced ESCs and astrocytes.

Distant organ breast cancer metastasis appears to rely on a specific subpopulation of ER- breast cancer cells. Triple negative MDA-MB231 breast cancer cells that disseminate to the lung, bone, liver, and brain are specific subclones (4). We have induced more than 10 distinct BCSC subtypes by stable NRF1 overexpression. These subtypes may have different tumor cell fates in establishing metastatic lesions. Although we have shown that NRF1-induced BCSCs form tumors in vivo, whether these cells pass through the blood brain barrier is not known. To determine if $BCSCs^{NRF1}$ pass through an in vitro blood-brain barrier model, we used human breast epithelial MCF-10A cell line as a negative control and MDA-MB231 cells as the positive control (Fig. 3). NRF1 induced MCF-10A cells or $BCSCs^{NRF1}$ and NRF1 induced MDA-MB231 breast cancer cells were tested for adhesion and invasion. As shown in Fig. 3, breast cancer cells (BCS) were grown on top of a brain endothelial cell (BEC) and astrocyte cell (AC) monolayer. The influence of NRF1 on cell adhesion was determined by measuring fluorescence of endothelialCD34 marker (in blue) and the BCSC marker CD133 (in red) using confocal microscopy. The upper left quadrant of Fig. 3A is the negative control showing only the blue marker for endothelial CD34 with no adhesion of BCSCs indicated by no red stained cells for CD133 marker. The lower left quadrant shows MDA-MB231 breast cancer cells with CD133 marker (in red) and endothelial cells (in blue). $BCSCs^{NRF1}$ showed a huge increase in adhesion to the endothelial layer compared to breast epithelial cells MCF-10A (Fig. 3A top right panel). NRF1 induced MDA-MB231 also showed increased cell adhesion

to the endothelial layer indicated by the CD133 marker in red compared to MDA-MB231 cells not transfected with NRF1 (Fig. 3A lower right panel). The increase in CD133 by MDA-MB231 cells expressing NRF1 also indicate these cells acquired a more mesenchymal phenotype. Together these results show that NRF1 expression improved endothelial adhesion by both BCSCs^{NRF1} and NRF1 induced MDAMB231 cells to the brain barrier model shown by pink, fluorescent cells where both CD133 and CD34 markers overlap. Since the high expression of CD133 in triple negative breast cancer cells correlates with high invasive potential (15), we determined if BCSCs^{NRF1} and NRF1 induced MDA-MB231 cells crossed the blood brain barrier model. Brain microvascular endothelial cells and astrocytes were seeded in a monolayer and invasion was determined by measuring cells that reached the bottom of the endothelial barrier. As shown in the top and lower left panels of Fig. 3B, MCF-10A cells did not migrate across the brain barrier model with no observed cells at the bottom of the well, however, the aggressive MDA-MB231 breast cancer cell line did migrate through the barrier. BCSCs ^{NRF1} and NRF1 induced MDA-MB231 breast cancer cells showed increased migration through the brain barrier model when compared to cells not overexpressing NRF1 (Fig. 3B top and lower right panels). After establishing that NRF1 increased the migration through the endothelial barrier model, we also determined if these cells could migrate through a 3D biogel matrix that mimics more physiological conditions. We embedded BCSCs^{NRF1} and NRF1 induced MDA-MB231 cells in the center of a solid 3D matrix embedded with endothelial cells shown by CD34 marker in blue (Fig. 3C). Confocal microscopy showed that BCSCs^{NRF1} and NRF1 expressing MDA-MB231 migrated away from the initial tumor spheroid by day 9 (Fig. 3C). In summary, NRF1 induced BCSCs and MDA-MB231 breast cancer cells show increased cell adhesion as well as cell migration through a brain barrier model. Moreover, these NRF1 expressing breast cancer cells can migrate from the tumor spheroid through a 3D endothelial barrier.

ID proteins have been considered topromote tumor-associated endothelial progenitor cell proliferation and mobilization (16). Therefore, we determined whether ESCs^{ID3} increased BCSCs tumor spheroid migration using a transwell brain barrier model. BCSC spheroids were seeded on top of a transwell insert containing an endothelial monolayer. As shown in Fig. 4A, BCSC spheroids were grown on top of the endothelial layer. Confocal microscopy showed that BCSC spheroids adhered or spreaded on top of both wildtype ECs and ESCs^{ID3} (Fig. 4A). Next, we determined the effect of ESCs^{ID3} on brain barrier migration of BCSCs using the transwell assay. NRF1 and NRF1+E2 induced BCSCs showed higher migration through the barrier composed of ESCs^{ID3} indicated by higher fluorescence intensity (in green) compared to wildtype ECs (Fig. 4B). In summary, our findings show that a endothelial barrier composed of ESCs^{ID3} increased the migration of BCSCs from a tumor spheroid.

Since ID3 has been shown to be a secreted angiogenic transcription factor (14), we determined whether exosomal ID3 enters BCSCs. Endothelial exosome was isolated from ESCs^{ID3} cultures and used to treat BCSCs (Fig. 5). Western blots from cell lysates of BCSCs and ECs treated with endothelial exosome showed the highest level of ID3 found in ESCs (positive control). Treatment of wildtype ECs with endothelial exosome did not increase ID3 protein levels compared to no treatment. BCSCs treated with endothelial exosome did show an increase in ID3 protein level treatment when compared to untreated

BCSCs. These results suggest that exosomal ID3 enters BCSCs. To confirm our results, we measured the effects of endothelial exosome treatment in BCSCs by flow cytometry. As shown in Fig. 6 row A, less than 1% of the wildtype ECs population expressed ID3 which was increased to 5% after treatment with endothelial exosome. Exosomal treatment of BCSCs increased the combined expression of both ID3 and NRF1 positive cells in the $BCSC^{NRF1}$ population to 35%; and in BCSCs $^{NRF1+E2}$ to 40% (Fig. 6 rows B, C). These results confirm our Western blot results showing increased ID3 protein levels in BCSCs treated with endothelial exosome. In summary, exosomal treatment from $ESCs^{ID3}$ increased the protein level of ID3 in BCSCs and may help explain the paracrine effect of ESCs in supporting BCSCs adhesion and migration.

After observing that exosomal treatments increased protein levels of ID3 in BCSCs, we determined the phenotypic changes to BCSCs treated with endothelial exosome derived from ESCs in a tumor spheroid assay. BCSCs were grown in serum free media plus exosomal treatment shown in Fig. 7. At 10 days, BCSCs with exosome treatment formed tumor spheroids when co-cultured with wildtype ECs. These findings suggest a paracrine mechanism of ID3 contributing in promotion of tumorosphere growth of BCSCs.

ID proteins have been reported to facilitate breast cancer metastatic colonization of the lung and brain (6; 16). To validate our in vitro findings, we determined whether ESCs guided BCSCs in vivo and whether this migration was exacerbated by exposure to PCB153. Xenotransplantation of $ESCs^{ID3}$ in the zebrafish embryo (2dpf) was used to determine in vivo if ESCs had increased migration upon treatment with PCB153 (Fig. 8). ESCs were measured by confocal microscopy using GFP tracking of stable ID3 overexpressing endothelial stem cells as well as using red fluorescent dye, CellTracker™ CM-DiI (which stains both GFP and non-GFP labeled cells). The treatment of these cells with PCB153 showed more GFP fluorescent dye labeled ECs moved through blood vessels from the site of injection (yolk) to the region of secondary target organs compared to non-treated cells. This demonstrated the potential for $ESCs^{ID3}$ to guide BCSCs in vivo and its potential to contribute to metastatic lesions. Therefore, we determined the metastatic potential of BCSCs in the presence and absence of brain $ESCs^{ID3}$. As shown in Fig. 9 bottom panel, $ESCs^{ID3}$ guided NRF1+E2-induced BCSCs to form a xenograft tumr in the neural crest when compared to no ESCs (2^{nd} and 3^{rd} row).

Discussion

Distant organ breast cancer metastasis appears to rely on a specific subpopulation of BCSCs (4). Therefore, we determined if NRF1 induced BCSCs could cross a model of the blood brain barrier as well as the contribution of ID3-induced endothelial stem cells in guiding BCSCs across this barrier. The major novel findings from our study include: NRF1 induced BCSCs cross a blood brain barrier model and form xenograft tumors in the zebrafish neural crest. ID3-induced endothelial stem cells increased the migration of BCSCs through an in vitro blood brain barrier as well as the in vivo migration of BCSCs. And treatment with endocrine disrupting chemical PCB153 and exosomal ID3 increased BCSC tumor spheroid growth. These findings show for the first time a key role of ID3 in guiding circulatory endothelial stem cells to

accompany NRF1-induced BCSCs to distant metastatic sites where they most likely facilitate the seeding, survival, and proliferative capacity of BCSCs. These findings will help in setting the stage for pre-clinical testing of NRF1/ID3 modifying agents that prevent the metastatic spread of breast cancer.

Estrogen has important biological actions in non-reproductive organs. The liver, lung, brain, and bone are not only major secondary target sites of estrogen receptor negative (ER-) breast cancer, but are also estrogen enriched tissues because they locally synthesize estrogen by aromatization (17, 18). Environmental estrogenic chemicals accumulating in human breast are suspected to contribute to both breast cancer risk and metastases to distant organs (19, 20). Polychlorinated biphenyls (PCBs), a class of chlorinated compounds ubiquitous in the environment, were classified as a Group 1 carcinogen (i.e., carcinogenic to humans) in 2013 by the International Agency for Research on Cancer. Sex-dependent accumulation of PCBs, including PCB153, has been reported in post-mortem female brain tissue while experimental evidence from animal models show selective accumulation of PCB153 in the brain and lung (21). Levels of PCBs in various human tissues, including the breast are strongly associated with age, reflecting long-term environmental exposure and bioaccumulation (22). Elevated PCB levels in breast adipose tissues have been linked to an increased rate of breast cancer recurrence (23). PCBs have also been shown to enhance metastatic properties of breast cancer cells (24). The brain, bone, and lung are exposed to peak estrogen levels during the follicular phase in pre-menopausal women and in the absence of ovarian estrogens these organs locally synthesize estrogen by aromatase (17). Triple negative (ER-, PR-, HER2-) and HER2 + breast cancers are more prevalent in pre-menopausal women; and young age (< 40 year) is an independent risk factor for brain metastasis (25). Distant organ breast cancer metastasis appears to rely on a specific subpopulation of ER- BCSCs. For instance, triple negative MDA-MB231 breast cancer cells that disseminate to the lung, bone, liver, and brain in NOD-SCID mice are specific subclones of the parental line with a particular cell surface marker signature (4). Despite these evidences, the role of estrogenic chemicals in the increased specification and guidance of ER – breast cancer to spread to secondary organs represents a critical gap in knowledge. Patients with ER- breast cancer are not given anti-estrogen therapy because it has been assumed to be ineffective. This has led to a critical barrier in which current therapy cannot reverse the spread and colonization of breast cancer to distant organs.

Key observations performed in our laboratory led us to identify that exposure to 17β-estradiol (E2) and PCB153 activate growth-regulating genes by astrocytes and endothelial cells surrounding brain or lung metastases (8;19,20,26). The significance of our discovery is that breast tumor cells colonizing these organs may advantageously hijack the available local estrogen as well as PCBs for growth. Our studies support a novel concept that ID3 expressing vascular endothelial stem cells are not just contributing in new blood vessel formation, but also increased the adhesion and migration of BCSCs. During blood-borne metastasis, upregulation of endothelial cell adhesion molecules can accelerate metastatic processes of BCSCs through increased adhesion of tumor cells to the endothelium. We have reported that physiological levels of E2 and estrogenic PCB153 [1ng/ml], a dose found in human serum [0.60–1.63 ng/ml], altered endothelial cell phenotypes (8). PCB153's effects on vasculosphere formation and vessel sprouting were more pronounced than E2. Expression of ID3, a transcription regulator, has been reported

to be significantly associated with breast tumorigenesis in large cohorts of human breast cancer (6). High expression of ID3 was demonstrated to drive both tumor initiation at the primary site as well as colonization at lung metastatic sites in triple negative breast tumors (6). Until now, the role of ID3 has been limited to the process of tumor angiogenesis. In our study, differential effects were demonstrated with endocrine disruptors PCB153 and PCB77. PCB153 treatment exacerbated migration of NRF1 induced BCSCs. PCB153 also increased tumor cell adhesion to microvascular endothelium and transendothelial migration of BCSCs. $ESCs^{ID3}$ not only supported the growth of BCSC tumor spheroids, but guided the in vivo migration of tumor stem cells to the neural crest in the zebrafish embryo. These studies provide convincing support to our postulate that gain-of-function by NRF1 in BCSCs and ID3 in ESCs will lead to guidance of BCSCs to spread to distant sites in exposed individuals. Moreover, the effect of environmental pollutant PCB153 has expanded our understanding of how environmental exposure to endocrine disruptors may influence the specification of $BCSCs^{NRF1}$ and their guidance by $ESCs^{ID3}$ to secondary target organs. Thus, establishing a role for NRF1/ID3 in guidance of BCSCs to spread to secondary target organs will directly link environmental exposures and breast cancer metastasis because both NRF1 and ID3 are activated or antagonized by a variety of drugs and environmental estrogenic chemicals, including PCB153.

In summary, the major novel findings of this study illustrate new roles of NRF1 and ID3 in the invasiveness of BCSCs. These findings show for the first time a key role for ID3 and NRF1 by which specific circulatory endothelial stem cells may accompany BCSCs to distant metastatic sites to facilitate the seeding, survival, and proliferative capacity of BCSCs. Findings of this study provide not only a new understanding for the mechanism of how both environmental exposures may support breast cancer metastasis but also important information for the design of a new therapy for BCSCs for the prevention and treatment of estrogen-dependent breast cancer.

Declarations

Acknowledgements:

This research is supported in part by the NIH R15 Award (1R15HL145652-01).

References

1. Ramos J, Das J, Felty Q, Yoo C, Poppiti R, Murrell D, Foster PJ, Roy D. NRF1 motif sequence-enriched genes involved in ER/PR -ve HER2 +ve breast cancer signaling pathways. Breast Cancer Res Treat. 2018 Nov;172(2):469-485. doi: 10.1007/s10549-018-4905-9. Epub 2018 Aug 20. PMID: 30128822.
2. Das JK, Felty Q, Poppiti R, Jackson RM, Roy D. Nuclear Respiratory Factor 1 Acting as an Oncoprotein Drives Estrogen-Induced Breast Carcinogenesis. Cells. 2018 Nov 27;7(12):234. doi: 10.3390/cells7120234.

3. Li F, Tiede B, Massagué J, Kang Y. Beyond tumorigenesis: cancer stem cells in metastasis. Cell Research. 2007;17(1):3–14.
4. Ghajar CM, Peinado H, Mori H, et al. The perivascular niche regulates breast tumour dormancy. Nat Cell Biol. 2013;15(7):807-817. doi:10.1038/ncb2767
5. Chen YH, Wu ZQ, Zhao YL, Si YL, Guo MZ, Han WD. FHL2 inhibits the Id3-promoted proliferation and invasive growth of human MCF-7 breast cancer cells. Chin Med J (Engl) 125: 2329 –2333, 2012.
6. Gupta GP, Perk J, Acharyya S, de Candia P, Mittal V, TodorovaManova K, Gerald WL, Brogi E, Benezra R, Massagué J. ID genes mediate tumor reinitiation during breast cancer lung metastasis. Proc Natl Acad Sci USA 104: 19506 –19511, 2007.
7. Felty Q, Porther N. Estrogen-induced redox sensitive Id3 signaling controls the growth of vascular cells. Atherosclerosis. 2008 May;198(1):12-21. doi: 10.1016/j.atherosclerosis.2007.12.048. Epub 2008 Feb 20. PMID: 18281048.
8. Das JK, Felty Q. PCB153-induced overexpression of ID3 contributes to the development of microvascular lesions. PLoS One. 2014 Aug 4;9(8):e104159. doi: 10.1371/journal.pone.0104159. PMID: 25090023; PMCID: PMC4121297.
9. Das JK, Felty Q. Microvascular lesions by estrogen-induced ID3: its implications in cerebral and cardiorenal vascular disease. J Mol Neurosci. 2015 Mar;55(3):618-31. doi: 10.1007/s12031-014-0401-9. Epub 2014 Aug 17. PMID: 25129100; PMCID: PMC4320014.
10. Das JK, Voelkel NF, Felty Q. ID3 contributes to the acquisition of molecular stem cell-like signature in microvascular endothelial cells: its implication for understanding microvascular diseases. *Microvasc Res*. 2015;98:126-138. doi:10.1016/j.mvr.2015.01.006
11. Urano Y, Fukushima T, Kitamura S, Mori H, Baba K, Aizawa S. Statistical studies on metastasis of breast cancer and cancer metastasis to the breast. *Gan No Rinsho.* 1986;Suppl:205–223.
12. Naik RP, Jin D, Chuang E, Gold EG, Tousimis EA, Moore AL, Christos PJ, de Dalmas T, Donovan D, Rafii S, Vahdat LT. Circulating endothelial progenitor cells correlate to stage in patients with invasive breast cancer. Breast Cancer Res Treat. 2008 Jan;107(1):133-8. doi: 10.1007/s10549-007-9519-6. Epub 2007 Feb 15. PMID: 18043899.
13. Nishi M., Sakai Y., Akutsu H., Nagashima Y., Quinn G., Masui S., Kimura H., Perrem K., Umezawa A., Yamamoto N., et al. Induction of cells with cancer stem cell properties from nontumorigenic human mammary epithelial cells by defined reprogramming factors. Oncogene. 2014;33:643–652. doi: 10.1038/onc.2012.614.
14. Isozaki, T., Amin, M.A., Arbab, A.S. et al. Inhibitor of DNA binding 1 as a secreted angiogenic transcription factor in rheumatoid arthritis. Arthritis Res Ther 16, R68 (2014). https://doi.org/10.1186/ar4507
15. Brugnoli, F., Grassilli, S., Piazzi, M. et al. In triple negative breast tumor cells, PLC-β2 promotes the conversion of CD133high to CD133low phenotype and reduces the CD133-related invasiveness. Mol Cancer 12, 165 (2013). https://doi.org/10.1186/1476-4598-12-165

16. Nair R, Teo WS, Mittal V, Swarbrick A. ID proteins regulate diverse aspects of cancer progression and provide novel therapeutic opportunities. *Mol Ther*. 2014;22(8):1407-1415. doi:10.1038/mt.2014.83
17. Barakat R, Oakley O, Kim H, Jin J, Ko CMJ. Extra-gonadal sites of estrogen biosynthesis and function. BMB Rep. 49(9): 488-496, 2016.
18. Nelson LR, Bulun SE. Estrogen production and action. J Am Acad Dermatol. 45(3 Suppl):S116-24, 2001.
19. Roy D, Morgan M, Yoo C et al. Integrated bioinformatics, environmental epidemiologic and genomic approaches to identify environmental and molecular links between endometriosis and breast cancer. Int. J. Mol. Sci. 16(10), 25285-25322, 2015
20. Morgan M, Deoraj A, Felty Q, Roy D. Environmental estrogen-like endocrine disrupting chemicals and breast cancer. Mol Cell Endocrinol. pii: S0303-7207(16)30411-7, 2016.
21. Hatcher-Martin JM, Gearing M, Steenland K, Levey AI, Miller GW, Pennell KD. Association between polychlorinated biphenyls and Parkinson's disease neuropathology. Neurotoxicology. 33(5):1298-304, 2012.
22. Chu S, Covaci A, Schepens P. Levels and chiral signatures of persistent organochlorine pollutants in human tissues from Belgium. Environ Res. 93(2):167-76, 2003.
23. Muscat JE, Britton JA, Djordjevic MV et al. Adipose concentrations of organochlorine compounds and breast cancer recurrence in Long Island, New York. Cancer Epidemiology, Biomarkers & Prevention 12, 1474–1478, 2003
24. Liu S, Li S, Du Y. Polychlorinated biphenyls (PCBs) enhance metastatic properties of breast cancer cells by activating Rho-associated kinase (ROCK) PLoS ONE. 2010;5:e11272.
25. Sartorius CA, Hanna CT, Gril B. et al. Estrogen promotes the brain metastatic colonization of triple negative breast cancer cells via an astrocyte-mediated paracrine mechanism. Oncogene 35, 2881-2892, 2016
26. Perciados M, Yoo C, Roy D. Estrogenic endocrine disrupting chemicals influencing NRF1 regulated gene networks in the development of complex human brain diseases. Int. J. Mol. Sci. 17(12), 2086, 2016.

Figures

Figure 1

Exposure to PCB congeners increased spheroid formation of BCSCs co-cultured with ESCs and astrocyte cells. Tumor spheroid assay 16 days after exposure to PCB congeners. A) Wild-type brain microvascular endothelial cells shown by endothelial CD34 marker (in blue). B) NRF1 induced BCSCs expressing GFP (in green). C) NRF1 induced BCSCs co-cultured with endothelial cells. D-E) Astrocyte cells (AC) co-cultured with BCSCs and wildtype ECs. Astrocyte marker GFAP is shown in red. F) Astrocyte cells co-cultured with

BCSCs and ID3 induced ESCs (in green). Representative confocal microscopy images from three separate experiments. 200X. PCB77 [60uM]; PCB153 [60uM]

Figure 2

ID3 induced endothelial stem cells support the growth of BCSC spheroids. Spheroid assay of BCSCs^{NRF1} co-cultured with wildtype ECs or ESCs^{ID3}. Cells were treated with vehicle control, PCB77 or PCB153 and grown for 8 to 16 days. A) Wild-type brain microvascular endothelial cells. B) NRF1 induced BCSCs. C) NRF1 induced BCSCs cultured with wildtype ECs. D) NRF1 induced BCSCs cultured with ECs and astrocyte cells (ACs). E) NRF1 induced BCSCs cultured with ESCs and astrocyte cells. Representative light microscopy images from three separate experiments. F) Graphs of spheroid diameter for groups A-E. PCB congener treatment exhibited a significant increase in spheroid diameter at days 8 and 16 when compared to vehicle control. Error bars represent the mean sizes of fifteen spheroids ± SD. * $p<0.05$ ** $p<0.01$ vs. Control. Data analyzed by ANOVA; Tukey HSD test for multiple comparisons.

Figure 3

NRF1 increased adhesion and migration of breast cancer cells. A) BCSCs^{NRF1} and NRF1-induced MDA-MB231 were seeded on top of a brain barrier model in serum-free media for 3 days. Adhesion to the endothelial layer is shown by CD34 marker (in blue) and CD133 marker (in red) for BCSCs and NRF1-induced mesenchymal MDA-MB231 cells. Pink, fluorescent cells show where both CD133 and CD34 markers overlap. B) Invasion of BCSCs^{NRF1} and NRF1-induced mesenchymal MDA-MB231 through the brain barrier. C) 3D brain barrier model composed of NRF1-induced breast cancer cells (CD133 in red)

surrounded by a Matrigel of endothelial cells (CD34 in blue) at day 0 (D0). BCSCs^{NRF1} top panel and NRF1-induced MDAMB231 cells lower panel. Migration of CD133 positive cells away from the tumor spheroid shown in magnified images at day 9 (D9). Representative confocal microscopy images from three separate experiments.

Figure 4

ID3 induced endothelial stem cells increase BCSCs migration. A) BCSCs tumor spheroids seeded on a monolayer of wildtype ECs or ESCs^{ID3}. BCSCs were induced by either NRF1 or NRF1+E2. Wildtype ECs stained with CD34 in blue. ESCs^{ID3} stained with anti-ID3 in red. B) BCSCs^{NRF1} spheroids were seeded on an endothelial monolayer for 24h in serum-free media in the upper chamber of a transwell insert with FBS as a chemoattractant in lower chamber. NRF1 overexpressing cells shown by GFP in green were photographed in the lower chamber. Representative confocal microscopy images from three separate experiments.

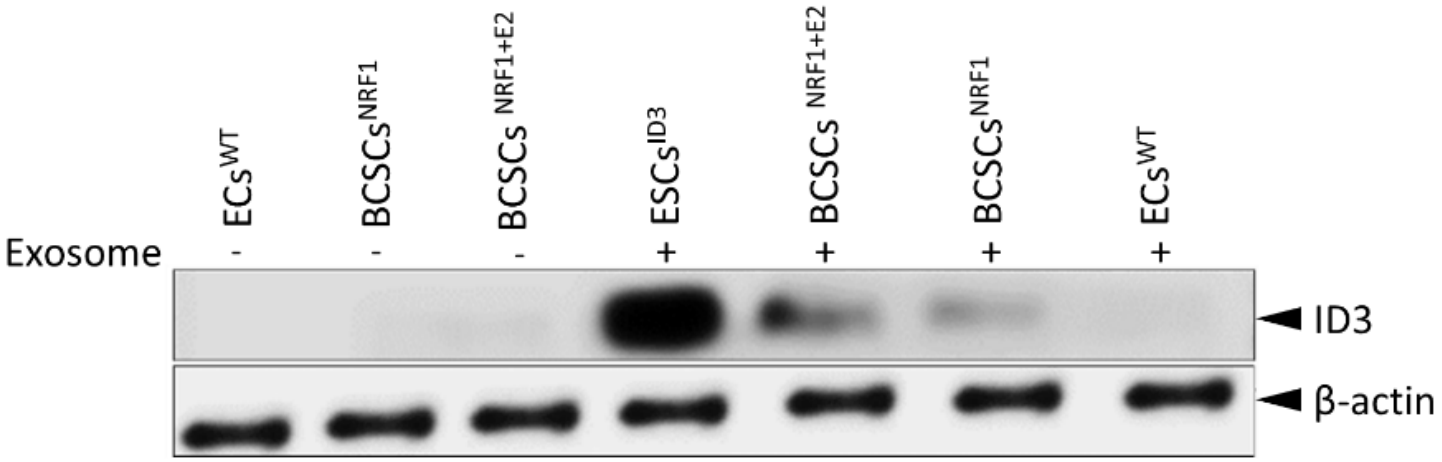

Figure 5

Endothelial exosome treatment increases ID3 protein level in BCSCs. BCSCs were treated with endothelial exosomes from ESCs^{ID3} for 24 h. BCSCs were induced by either NRF1 or NRF1+E2. BCSCs showed increased ID3 protein levels from exosome treatment. Representative Western blot of 3 separate experiments. ID3 levels shown in top panel with loading control on bottom.

Figure 6

Flow cytometry analysis of BCSCs treated with endothelial exosome. FACS analysis using ID3 biotin-FITC (pink) and NRF1 conjugated PE (blue). Co-expression of ID3 and NRF1 shown in green. Cells not expressing either marker shown in red. A) Wildtype endothelial cells. B) NRF1 induced BCSCs. C) NRF1 + E2 induced BCSCs. D) ESCs ^{ID3} (positive control). BCSCs were induced by either NRF1 or NRF1+E2.

Figure 7

Endothelial exosome treatment BCSCs tumor spheroids. Spheroid assay of NRF1 induced BCSCs co-cultured with wildtype ECs. Cells were treated with endothelial exosome from ESCs in serum free media for 7 – 10 days. BCSCs are shown by CD133 marker in red and WT-EC are shown by CD34 marker in blue.

Figure 8

PCB153 increased in vivo migration of lung ESCs. Top panel show lung ESCs^{ID3} xenotransplanted in zebrafish embryo (2dpf). Bottom panel showing PCB153 [60uM] treated lung ESCs xenotransplanted into the zebrafish. Total number of injected cells are shown by red fluorescent dye CellTracker™ CM-DiI and ID3 overexpressing cells indicated by GFP (in green). Representative images from 3 individual experiments.

Figure 9

BCSCs form xenograft tumor in neural crest of zebrafish embryo. Total number of injected cells are shown by red fluorescent dye CellTracker™ CM-DiI and NRF1 overexpressing BCSCs indicated by GFP (in green). Top panel represents ID3 induced ESCs (GFP expressing) xenotransplanted in zebrafish embryo (2dpf). Row two represents NRF1 induced BCSCs. Row three represents NRF1+E2 induced BCSCs. Bottom panel represents NRF1+E2 induced BCSCs and ESCs. Representative images of 3 individual experiments.